



RESEARCH ARTICLE

THE LUMINESCENCE AND THERMOLUMINESCENCE STUDIES OF Nd³⁺ DOPED
Sr₂SiO₄

Tuncay YEŞİLKAYNAK^{1,*} , Ruken Esra DEMİRDÖĞEN² ,
Vural Emir KAFADAR³ , Fatih Mehmet EMEN⁴ 

¹ Department of Chemistry Technology, Afsin Vocational School, Kahramanmaraş Sütcü İmam University, TR46500, Kahramanmaraş, Turkey

² Department of Chemistry, Faculty of Science, Cankiri Karatekin University, TR-18100, Cankiri, Turkey

³ Gaziantep University, Department of Engineering Physics, Gaziantep, Turkey

⁴ Department of Chemistry, Faculty of Arts and Science, Burdur Mehmet Akif Ersoy University, TR-15100, Burdur, Turkey

ABSTRACT

Sr₂SiO₄:%3Nd³⁺ was synthesized and its structural characterization was made via XRD technique. The results indicated that Sr₂SiO₄:%3Nd³⁺ had Pm3m (62) space group (PDF: 00-039-1256) in the orthorhombic crystal system. Luminescence and thermoluminescence (TL) properties of Sr₂SiO₄:%3Nd³⁺ was investigated in detail. Computerized glow curve deconvolution methods was used for to determine the kinetic properties of Sr₂SiO₄:%3Nd³⁺. The TL results showed that Sr₂SiO₄:Nd³⁺ consisted of seven TL glow peaks.

Keywords: Phosphors, Silicates, Hydrothermal synthesis, SrSiO₄

1. INTRODUCTION

Inorganic luminescent materials or the phosphors, which have been known for more than a hundred years but gained much importance since they are necessary for lighting and display systems as they recently started to be used as light-emitting diodes [1]. Phosphors doped with Nd³⁺ ions, which constitute an important class of inorganic luminescent materials, is based on aluminates and alkaline earth silicates- the most important rare-earth minerals and source of rare-earth elements [1,2]. However, thermoluminescent properties of Sr₂SiO₄:Nd³⁺ still await to be elucidated. The favorable properties of thermoluminescence (TL) dosimeters (i.e., high sensitivity, small sizes, capability of making point dose measurements, variety of forms, cost-effectiveness) render them useful in various radiation fields such as personal and environmental monitoring, as various dosimeters (retrospective, medical, space and high-dose dosimetry) [3]. Different forms of barium silicate obtained by different methods is much used by researchers as host material in thermoluminescence studies. Yamaga et al. studied barium silicate (Ba₂SiO₄) and (Ba₃SiO₅) doped by Eu²⁺. Ba₂SiO₄ radiated with UV light and the broadband luminescence of (Ba₂SiO₄) and (Ba₃SiO₅) produced peak wavelengths of 510 and 590 nm, respectively. Yamaga et al reported that upon UV excitation electrons and holes were produced in the crystal via thermal hopping and tunneling moved back to Eu²⁺ sites where Eu²⁺ recombined radiatively [4]. In 2010, Yao et al., who studied the photoluminescence properties of Ba₂ZnSi₂O₇:Eu²⁺,Re³⁺ (Re = Dy, Nd) prepared via the combustion-assisted synthesis (CAS) technique, reported that the single band centered at 503 nm in the emission spectrum corresponding to the 4f⁶5d¹ → 4f⁷ transition of Eu²⁺ is obtained when Dy³⁺ and Nd³⁺ ions were doped into Ba₂ZnSi₂O₇:Eu phosphors giving blue-green afterglow with emission wavelength at λ_{em} = 503 nm [5].

The bluish-green long-lasting phosphorescent phosphor obtained from N contained $\text{Ba}_2\text{SiO}_4:\text{Eu}^{2+}$ by Wang et al in 2010 was used for X-ray and cathode-ray tubes. This study reported that increasing the content of Si_3N_4 the phosphorescence grew super-linearly and some new TL peaks appeared at temperatures as low as 335, 355, 365, and 400 K which were attributed to the newly formed traps occurring due to N substitution for O [6]. Only in 2011 Sakamoto et al. achieved growing single crystal of $\text{Ba}_2\text{SiO}_4:\text{Eu}^{2+}$ via a new synthesis method in which SiO -included in the gas phase- and Ba–Sc–Al–Eu–O -in the solid phase- were hybridized to give $\text{Ba}_2\text{SiO}_4:\text{Eu}^{2+}$ single crystal. Interfacial crystal growth was achieved when the SiO gas was reacted with the surface of Ba–Sc–Al–Eu–O substrate in a reductive atmosphere. The size of the single crystals was reported to be $\sim 500 \mu\text{m}$ and they emitted green light at $\sim 500 \text{ nm}$ when excited at 300-450 nm [7]. In 2013, Huayna et al. reported $\text{Ba}_2\text{SiO}_4:\text{M}$ ($\text{M}=\text{Eu}^{3+}, \text{Eu}^{2+}, \text{Sr}^{2+}$) which had red, green, and blue photoluminescence [8].

In this study, $\text{Sr}_2\text{SiO}_4:\text{Nd}^{3+}$ was synthesized by hydrothermal method and indexed. its XRD pattern as orthorhombic crystal system with Pmmm space group (PDF:00-039-1256). The TL glow curves of $\text{Sr}_2\text{SiO}_4:\text{Nd}^{3+}$, which was obtained upon irradiating with 12 Gy beta-ray irradiation. The glow peaks of the curves, which had main glow peak at $\sim 175 \text{ }^\circ\text{C}$ and a shoulder at $\sim 300 \text{ }^\circ\text{C}$, can be observed due to the defects. The CGCD method was used to evaluate the trap parameters especially the activation energy (Ea) and the order of the kinetics (b).

2. MATERIAL METHOD

Strontium nitrate, neodymium (III) oxide, citric acid and ethanol with purity $\geq 99.9\%$ and polyethylene glycol 10 000 (100%) were purchased from Merck and were used as received without further purification. 3% Nd^{3+} -doped strontium silicate was obtained by Hydrothermal Method. $\text{Sr}(\text{NO}_3)_2$ solution obtained by dissolving 2×10^{-3} moles of the reagent in 15 mL deionized water and 1×10^{-3} moles of $\text{SiO}_2 \cdot x\text{H}_2\text{O}$ in deionized water or TEOS at a molar ratio at twice the molar ratio of polyethylene glycol dissolved in 15 mL ethanol and 0.2 g citric acid dissolved in 10 mL deionized water were obtained separately. Solution of neodymium (III)nitrate hydrate was obtained by dissolving it in 5 mL deionized water. Upon mixing the solutions of the metal salts with citric acid solution $\text{Sr}(\text{NO}_3)_2$ solution was added under stirring with a magnetic stirrer at 25°C for 10 minutes. The pH of the homogeneous solution was adjusted to 12 with 5 mol/L NaOH via a pH meter and was placed in a Teflon reactor and was left to stand for 1 hour before being placed in the hydrothermal reactor and the reaction was carried out at $120 \text{ }^\circ\text{C}$ under high pressure for 12-18 hours. After completing the reaction the oven was slowly cooled to room temperature (RT). The precipitate thus obtained was separated by centrifugation and was dried at $60 \text{ }^\circ\text{C}$ for 12 hours. $\text{Sr}_2\text{SiO}_4:\text{Nd}^{3+}$ was calcined at $1300 \text{ }^\circ\text{C}$ for 3 hours.

Structural characterization of $\text{Sr}_2\text{SiO}_4:\text{Nd}^{3+}$ was made by XRD in the diffraction angle range $20^\circ \leq 2\theta \leq 70^\circ$ using a 0.021° step with 20 kV at 40 mA, $\text{CuK}\alpha$ (1.54 Å) incident radiation. The morphology of the phosphor was determined by a LEO440 Computer Controlled Digital Scanning Electron Microscope. The photoluminescence (PL) spectra were obtained via a Varian Cary Eclipse Fluorescence spectrophotometer at room temperature and excitation and emission slits were arranged as 20 and 10, respectively. $\text{Sr}_2\text{SiO}_4:\text{Nd}^{3+}$ was irradiated at room temperature by a beta source from a calibrated emitter $90\text{Sr}-90\text{Y}$. Sr–90 obtained from daughter products ($90\text{Sr} \beta- 8.73 \times 10^{-14} \text{ J}$ together with $90\text{Y} \beta-3.63 \times 10^{-13} \text{ J}$) emits high energy beta particles (0.04 Gy/s). Harshaw QS 3500 TLD reader system -a manual type reader computer interfaced to hand operator- was used to read out the irradiated sample. The TLD reader system and program ran on WinREMS.

3. RESULT and DISCUSSION

The XRD powder pattern of $\text{Sr}_2\text{SiO}_4:\%3\text{Nd}^{3+}$ is given in Figure 1. The XRD peaks match with the structure of Sr_2SiO_4 (PDF: 00-039-1256). The crystal structure of $\text{Sr}_2\text{SiO}_4:\%3\text{Nd}^{3+}$ is determined to be orthorhombic crystal system with Pmma (62) space group. The unit cell parameters were $a = 7.0790 \text{ Å}$,

$b = 5.672 \text{ \AA}$, $c = 7.443 \text{ \AA}$; $\alpha = \beta = \gamma = 90^\circ$. No significant change was observed in the crystal structure of Sr_2SiO_4 when doped with 3% Nd^{3+} . In the eightfold coordination, the ionic radius of Nd^{3+} (1.109 Å) and Sr^{2+} (1.26 Å) were close to each other. However, the ionic radius of Si^{4+} in the fourfold coordination is 0.26 Å. This is too small to host Nd^{3+} . Therefore, not the Sr^{4+} ions but the Si^{2+} are replaced with Nd^{3+} .

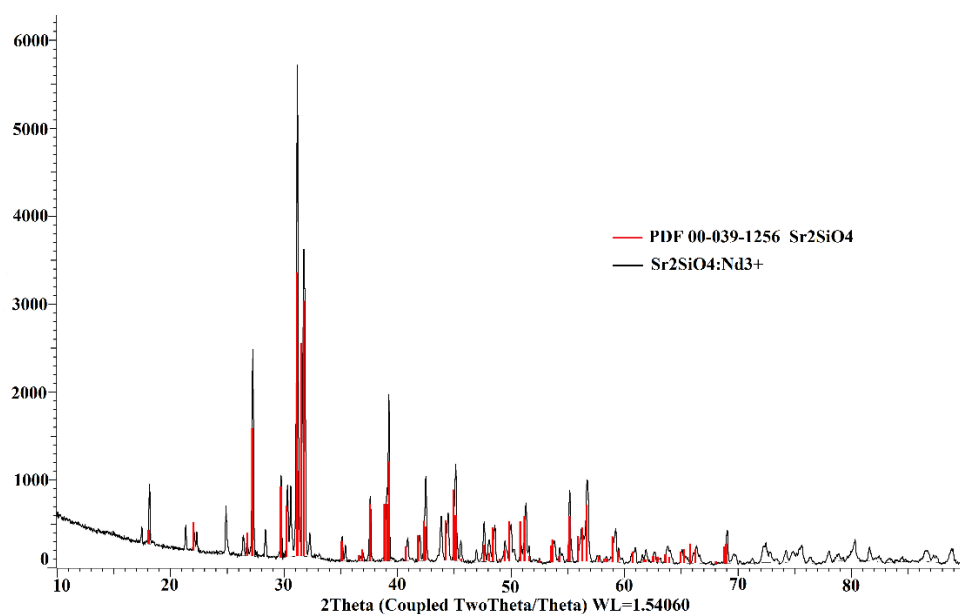


Figure 1. The XRD pattern of $\text{Sr}_2\text{SiO}_4:\text{Nd}^{3+}$

In Figure 2 can be seen the surface morphology of $\text{Sr}_2\text{SiO}_4:\text{Nd}^{3+}$ as investigated by SEM analysis. The average grain size of thus obtained $\text{Sr}_2\text{SiO}_4:\text{Nd}^{3+}$ was observed to be in the range of 230-650 nm in the SEM micrographs with 10000× magnification.

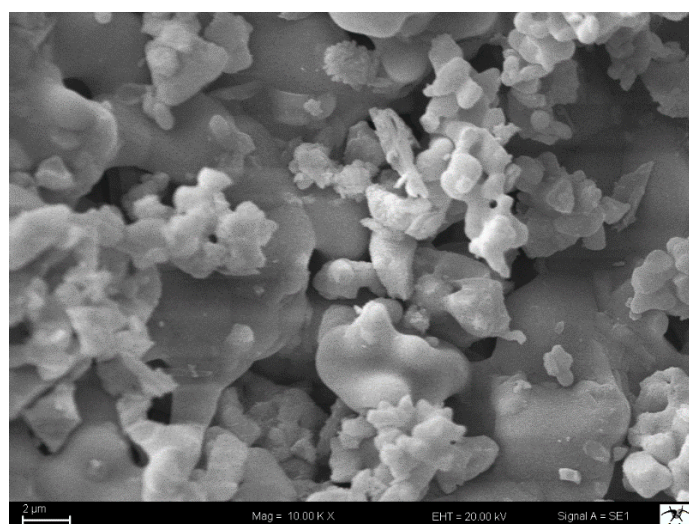


Figure 2. The SEM micrograph of $\text{Sr}_2\text{SiO}_4:\text{Nd}^{3+}$

In Figure 3 is given the excitation and emission spectra of $\text{Sr}_2\text{SiO}_4:\text{Nd}^{3+}$. The intense band observed at 295 nm in the excitation spectrum indicates overlapping of the electronic $\text{O}^{2-} \rightarrow \text{Nd}^{3+}$ transitions in the activator ion with the charge transfer (CT) transitions due to the $\text{O}^{2-} \rightarrow \text{Si}^{4+}$ transitions in the host crystal. Moreover, the weak excitation bands observed in the excitation spectrum in the range 295-400 nm

correspond to electron transitions of Nd^{3+} ions from ${}^6\text{H}_{15/2} \rightarrow {}^4\text{M}_{17/2}$ (295 nm) [9], ${}^6\text{H}_{15/2} \rightarrow {}^4\text{I}_{11/2}$ (352 nm) [10], ${}^6\text{H}_{15/2} \rightarrow {}^4\text{M}_{15/2}$ (360 nm) [10] and ${}^6\text{H}_{15/2} \rightarrow {}^6\text{P}_{7/2}$ (465 nm) [10,11]. In the emission spectrum due to ${}^4\text{I}_{9/2} \rightarrow {}^4\text{G}_{5/2}$ [12,13] and ${}^4\text{I}_{9/2} \rightarrow {}^4\text{G}_{7/2}$ transitions of Nd^{3+} ions intense emission bands were observed at 476 nm and 585 nm, respectively [12,13]. Moreover, due to ${}^4\text{F}_{9/2} \rightarrow {}^6\text{H}_j$ ($j = 11/2, 9/2$) transitions of Nd^{3+} ions low-intensity emission bands observed in the range from 665 to 760 nm [10].

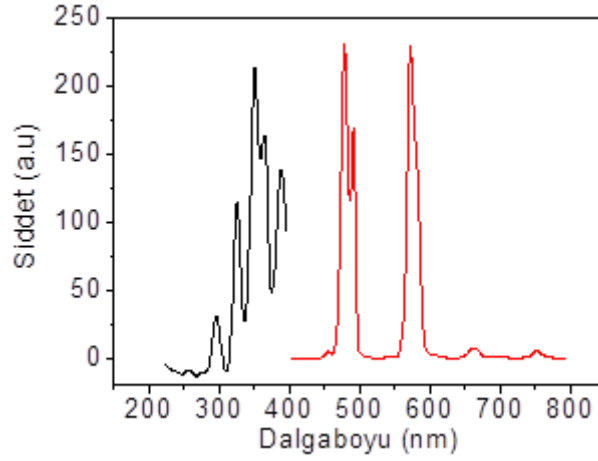


Figure 3. Excitation and emission spectra of $\text{Sr}_2\text{SiO}_4:\% \text{Nd}^{3+}$

The different TL glow curves obtained at different dosing periods of $\text{Sr}_2\text{SiO}_4:\text{Nd}^{3+}$ are given in Figure 4 which explicitly show gradual shift of the peak temperature to the higher temperature side with the increasing dose level. The peaks were observed to reach maximum intensity in the temperature range from 100 to 250°C at different dose levels. For Nd^{3+} -doped Sr_2SiO_4 , the CGCD method was used for to evaluate the trapping parameter of the main dosimeter peak of and for to determine the kinetic parameters (i.e., the number of glow peaks, activation energies (E_a), and kinetic order (b)) of the dosimetric peaks. Computerised glow curve deconvolution results for $\text{Sr}_2\text{SiO}_4:\%3\text{Nd}^{3+}$ are given Figure 5. In this study, different number of glow peaks were tried. It was observed that the glow curve structures of $\text{Sr}_2\text{SiO}_4:\text{Nd}^{3+}$ were well described by a linear combination of at least seven glow peaks since only then a reasonably good fit was obtained. In Table 1 are given the results of E_a , s , and b obtained via the CGCD methods [14].

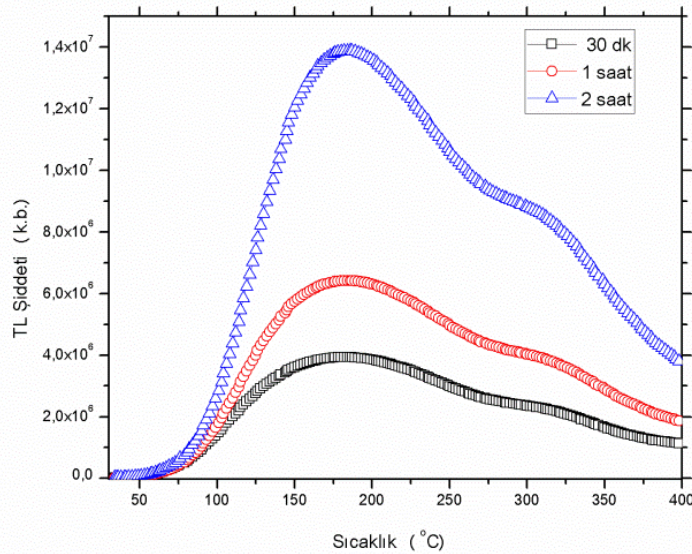


Figure 4. The thermoluminescence curves of $\text{Sr}_2\text{SiO}_4:\text{Nd}^{3+}$

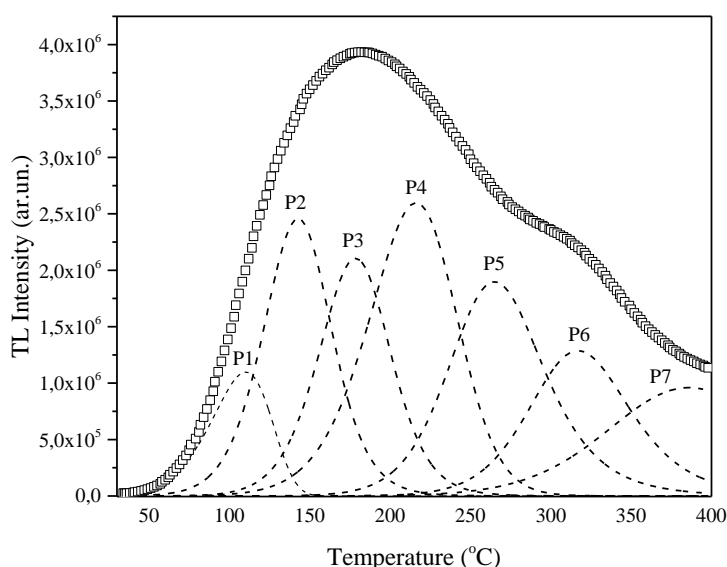


Figure 5. Computerised glow curve deconvolution results for Sr₂SiO₄:%3Nd³⁺ measured after 72 Gy irradiation by beta ray at room temperature ($\beta = 1 \text{ }^\circ\text{C}\cdot\text{s}^{-1}$) (FOM: 0,7)

With the approximation for $b \approx 1.1$ the below given general order kinetic analytical equation was used.

$$I(T) = I_m \cdot b^{b/b-1} \cdot \exp\left(\frac{E}{kT} \cdot \frac{T - T_m}{T_m}\right) \cdot [(b - 1) \cdot (1 - \Delta) \cdot \frac{T^2}{T_m^2} \cdot \exp\left(\frac{E}{kT} \cdot \frac{T - T_m}{T_m}\right) + Z_m]^{-b/b-1}$$

where;

$$\Delta = \frac{2kT}{E}, \quad \Delta_m = \frac{2kT_m}{E}, \quad Z_m = 1 + (b - 1) \cdot \Delta_m$$

Table 1. The trapping parameters of Nd³⁺ doped Sr₂SiO₄

	T _{max} (°C)	E (eV)	b
P1	109	0.62	1.00
P2	142	0.87	1.62
P3	178	0.98	1.60
P4	215	0.83	1.30
P5	264	1.17	2.00
P6	316	1.32	1.96
P7	384	0.93	2.00

4. CONCLUSION

This study, which targeted at preparing Sr₂SiO₄:Nd³⁺ via hydrothermal synthesis method and at elucidating the thermoluminescence (TL) properties and kinetic parameters (the order of kinetics (b), activation energy (E_a), and the frequency factor (s)) of Sr₂SiO₄:%3Nd³⁺ after 90Sr–90Y β irradiation. The Computerized Glow Curve Deconvolution (CGCD) method was used to do the quantitative analysis of the kinetic parameters. When the TL glow curves of Sr₂SiO₄:Nd³⁺ obtained in different dosing periods were examined, it was determined that it reached the maximum density in the temperature range of 100 to 250 °C. According to computerised glow curve deconvolution results, it was seen that there are seven glow peaks in the radiation curve calculated for Sr₂SiO₄:Nd³⁺.

ACKNOWLEDGEMENTS

This work was supported by Kahramanmaraş Sütçü İmam University Research Fund (BAP-project no:2015/2-31M).

CONFLICT OF INTEREST

The authors stated that there are no conflicts of interest regarding the publication of this article.

REFERENCES

- [1] Liu H, Guo S, Hao Y, Wang H, Xu B. Luminescent properties of Eu^{3+} and Sm^{3+} activated M_2SiO_4 (M=Ba, Sr and Ca) red-emitting phosphors for WLEDs. *Journal of Luminescence* 2012; 132: 2908-2912.
- [2] Emen FM, Altinkaya R, Kafadar VE, Avsar G, Yesilkaynak T, Kulcu N. Luminescence and thermoluminescence properties of a red emitting phosphor, $\text{Sr}_4\text{Al}_{14}\text{O}_{25}:\text{Eu}^{3+}$ *Journal of Alloys and Compounds* 2016; 681: 260–267.
- [3] Bhatt BC, Kulkarni MS. Thermoluminescent phosphors for radiation dosimetry. *Diffus Defect Data, Pt A* 2013; 347: 179–227.
- [4] Yamaga M, Masui Y, Sakuta S, Kodama N, Kaminaga K. Radiative and nonradiative decay processes responsible for long-lasting phosphorescence of Eu^{2+} -doped barium silicates. *Phys Rev* 2005; 71: 205102.
- [5] Yao S, Li Y, Xue L, Yan Y. Photoluminescence properties of $\text{Ba}_2\text{ZnSi}_2\text{O}_7: \text{Eu}^{2+}, \text{Re}^{3+}$ (Re= Dy, Nd) long-lasting phosphors prepared by the combustion-assisted synthesis method. *J Alloys Compd* 2010; 490: 200–203.
- [6] Wang M, Zhang X, Hao Z, Ren X, Luo Y, Wang X, Zhang J. Enhanced phosphorescence in N contained $\text{Ba}_2\text{SiO}_4: \text{Eu}^{2+}$ for x-ray and cathode-ray tubes. *Opt Mater* 2010; 32: 1042–1045.
- [7] Sakamoto T, Uematsu K, Ishigaki T, Toda K, Sato M. Development of gas-solid phase hybrid synthesis method of single crystal $\text{Ba}_2\text{SiO}_4: \text{Eu}^{2+}$. *Key Eng Mater* 2011; 485: 325–328.
- [8] Streit HC, Kramer J, Suta M and Wickleder C. Red, Green, and Blue Photoluminescence of $\text{Ba}_2\text{SiO}_4:\text{M}$ (M = $\text{Eu}^{3+}, \text{Eu}^{2+}, \text{Sr}^{2+}$). *Nanophosphors Materials* 2013; 6: 3079-3093.
- [9] Zhang ZW, Song AJ, Ma MZ, Zhang XY, Yue Y, Liu RP. A novel white emission in $\text{Ca}_8\text{MgBi}(\text{PO}_4)_7:\text{Dy}^{3+}$ single-phase full-color phosphor. *J Alloys Compd* 2014; 601: 231–233.
- [10] Zhu G, Wang Y, Wang Q, Ding X, Geng W, Shi Y. A novel White emitting phosphor of Dy^{3+} doped $\text{Ca}_{19}\text{Mg}_2(\text{PO}_4)_{14}$ for light-emitting diodes. *J Lumin.* 2014; 154: 246–250.
- [11] Zhang Z, Song A, Shen X, Lian Q, Zheng X. A novel white emission in $\text{Ba}_{10}\text{F}_2(\text{PO}_4)_6:\text{Dy}^{3+}$ single-phase full-color phosphor. *Mater Chem Phys.* 2015; 151: 345–350.
- [12] Liu F, Liu Q, Fang Y, Zheng N, Yang B, Zhao G. White light emission from $\text{NaLa}(\text{PO}_3)_4:\text{Dy}^{3+}$ single-phase phosphors for light-emitting diodes. *Ceram Int* 2015; 41: 1917–1920.

- [13] Mhlongo MR, Koao LF, Motaung TE, Kroon RE, Motloung SV. Analysis of Nd³⁺ concentration on the structure, morphology and photoluminescence of sol-gel Sr₃ZnAl₂O₇ nanophosphor. *Results in Physics* 2019; 12: 1786-1796.
- [14] Afouxenidis D, Polymeris GS, Tsirliganis NC, Kitis G. Computerised curve deconvolution of TL/OSL curves using a popular spreadsheet program. *Radiat Prot Dosim* 2012; 149: 363–370.